J. Membrane Biol. 164, 25–34 (1998)

The Journal of
Membrane
Biology

Electrophysiological Study of Chimeric Sodium Channels from Heart and Skeletal Muscle

I. Deschênes[1], L.-Q. Chen[2], R.G. Kallen[2], M. Chahine[1]

[1]Laval Hospital, Research Center, 2725, Chemin St.-Foy, St-Foy, Québec, Canada, G1V 4G5

[2]Department of Biochemistry and Biophysics, University of Pennsylvania School of Medicine, Philadelphia, PA 19104-6059, USA

Received: 20 January 1998/Revised: 19 March 1998

Abstract. The α-subunit cDNAs encoding voltage-sensitive sodium channels of human heart (hH1) and rat skeletal muscle (rSkM1) have been expressed in the tsA201 mammalian cell line, in which inactivation properties appear to be normal in contrast to *Xenopus* oocytes. A series of rSkM1/hH1 chimeric sodium channels has been evaluated to identify the domains of the α-subunits that are responsible for a set of electrophysiological differences between hH1 and rSkM1, namely, midpoints and slope factors of steady-state activation and inactivation, inactivation kinetics and recovery from inactivation kinetics and their voltage-dependence. The phenotype of chimeric channels in which each hH1 domain was successively introduced into a rSkM1 α-subunit framework confirmed the following conclusions. (i) The D4 and or/C-ter. are responsible for the slow inactivation of hH1 sodium channels. (ii) Concerning the other differences between rSkM1 and hH1: steady-state activation and inactivation, kinetics of recovery from inactivation, the phenotypes are determined probably by more than one domain of the α-subunit.

Key words: Rat skeletal muscle — Human heart — Chimeric channel — Expression — Cell line — Patch-clamp — Sodium channels

Introduction

Voltage-gated sodium channels are membrane proteins that play an essential role in the establishment and maintenance of cell excitability. The opening of the voltage-gated sodium channels is responsible for the upstroke of the action potential in excitable cells (Hodgkin & Huxley, 1952; Catterall, 1992; Kallen, Cohen & Barchi, 1993; Catterall, 1993; Noda, 1993). The cDNAs for various nonallelic isoforms have been cloned, expressed, and the channels studied electrophysiologically (Kallen et al., 1993). These experiments have revealed important electrophysiological and pharmacological differences between isoforms that correspond to expectations based on channel behavior when different isoforms are examined in their native tissues. As might be expected for different gene products, the brain and striated muscle channel subtypes have unique tissue distributions during brain, heart, and skeletal muscle development and in normal compared with denervated adult skeletal muscle (Westenbroek, Merrick & Catterall, 1989; Yang et al., 1991; Cohen, Mello & Yang, 1993).

NaChs are composed of one large α-subunit (1800–2000 residues) and one or more smaller β-subunits (~220 amino acids). Expression of the α-subunit alone yields conductances with most of the identifying properties of respective channel subtypes, including ion selectivity (Backx et al., 1992; Heinemann et al., 1992), toxin sensitivity (Frelin et al., 1986; Chen et al., 1992; Chahine et al., 1996*a*) and voltage-dependent activation and inactivation, consistent with the idea that the α-subunit forms the pore of the channel. Current models for the tertiary structure of the α-subunit propose four repeat domains (D1-D4), 250–300 amino acids each, arranged around a central pore. Each domain contains 6 transmembrane segments (S1–S6), one (S4) with a repeat motif $(\{R^+/K^+\}UZ)_n$ of $n = 4$, 5, 5–7 and 8 in domains D1, D2, D3 and D4, respectively, and where U and Z are hydrophobic amino acids. The S4 segment functions as the voltage-sensor (Auld et al., 1990; Larsson et al., 1996; Yang, George & Horn, 1996). Two additional short segments (SS1 and SS2, comprising the P region) within the extracellular S5-S6 loop probably fold back into the membrane to form part of the outer vestibule/ion-conducting pore (Backx et al., 1992; Catterall, 1992; Kallen et al., 1993; Catterall, 1993; Noda, 1993; Pérez-García et al.,

Correspondence to: M. Chahine

1996; Tsushima, Li & Backx, 1997). In addition recent mutagenesis studies showed that the DIII-DIV linker of the α-subunit forms the inactivation gate of sodium channels (West et al., 1992; Patton et al., 1992).

If various channel attributes are due to the differences in the structures of relatively localized regions of the channel proteins, one might be able to make assignments of function when chimeric channels derived from phenotypically different parent channels are examined. Conflicting results were published regarding the role of the β-subunit as a modulator of hH1 sodium channels (Makita, Bennett & George, 1994; Nuss et al., 1995*a*), however from the same cited studies it was accepted that the β-subunit modulates the kinetics of rSkM1 and hSkM1. In a recent study it was suggested that the S5–S6 loops of DI and DIV of the α-subunit from hSkM1 contribute to the β1 subunit-induced gating modulation of sodium channel (Makita, Bennett & George, 1996).

When expressed in a human cell line (human embryonic kidney HEK 293, tsA201), hH1 and rSkM1, which are only ~50% similar at the amino acid level, show characteristic electrophysiological and pharmacological differences that have been described for sodium channels examined in the corresponding native tissues (Gellens et al., 1992; Nuss, Tomaselli & Marbán, 1995*b*; Chahine et al., 1996*a*; Makielski et al., 1996; Chahine, Plante & Kallen, 1996*b*; Wang, George & Bennett, 1996). It is our goal to relate the structural differences between these channel isoforms to the divergent biophysical and pharmacological characteristics of the channels by studies of parent and chimeric α-subunits under the same experimental conditions and using the same voltage-clamp protocols.

Materials and Methods

Transfection of tsA201 Cell Line

The tsA201 cell line, a mammalian cell line derived from human embryonic kidney HEK 293 cells, was grown in high glucose DMEM, supplemented with 10% fetal bovine serum, 2 mM L-glutamine, penicillin (100 U/ml) and streptomycin (10 mg/ml) (Gibco BRL), in 5% CO_2 humid atmosphere incubator. Transfection of tsA201 cells grown to 40–50% confluence on 100 mm plates was made utilizing the calcium phosphate method (Margolskee, McHendry-Rinde & Horn, 1993) with the following modification: in order to facilitate the identification of individual transfected cells, we cotransfected with an expression plasmid for a lymphocyte surface antigen (CD8-a) (Jurman et al., 1994). We used 10 μg of cDNAs encoding for hH1, rSkM1 or chimeric channel sodium channels, and 10 μg of CD8. For patch-clamp experiments, the cells were used 2 to 3 days post transfection. We incubate the cells in a medium containing anti-CD8-coated beads for 2 min (Dynabeads M-450 CD8). The preparation of the beads was made according to the manufacturer (Dynal A.S., Oslo, Norway). Cells expressing CD8 on their surface fix the beads and are easily distinguishable from untransfected cells. The coding segments of rSkM1 (Trimmer et al., 1989) and hH1 (Gellens et al., 1992) were cloned into HindIII and XbaI sites of pcDNA I (Invitrogen) and plasmid DNA was purified using Qiagen columns (Qiagen).

Patch-Clamp Method

Macroscopic sodium currents from transfected cells were recorded using the whole-cell method of the patch-clamp technique (Hamill et al., 1981). Patch electrodes were made from 8161 Corning glass and coated with Sylgard® (Dow-Corning) to minimize their capacitance. A good voltage clamp was accomplished using low resistance electrodes (<2MΩ) and a routine series resistance compensation was performed to values >80% to minimize voltage-clamp errors. An Axopatch 200 patch-clamp amplifier was used with series resistance compensation. Sodium currents were leak corrected using Axopatch 200 leak subtraction. Typically, the steady-state passive membrane response to a voltage step is subtracted from the output. Voltage-clamp command pulses were generated by microcomputer using pCLAMP software v5.5 (Axon Instruments). Recorded membrane currents were filtered at 5 kHz. For whole-cell recording, the patch pipette contained (mM): 35 NaCl ; 105, CsF; 10, EGTA; and 10, Cs-HEPES (pH = 7.4). The bath solution contained (mM): 150, NaCl; 2, KCl; 1.5, $CaCl_2$; 1, $MgCl_2$; 10, glucose; and 10, Na-HEPES (pH = 7.4). The values of the gating data of hH1 and rSkM1 are different from Chahine et al., 1996 due to the liquid junction potential correction of −7 mV between patch pipette and bath solutions used in this study. Experiments were performed at room temperature, 22–23°C. To minimize the influence of time-dependent shifts in the steady-state inactivation curves, recordings for the hH1, rSkM1 and all the chimeras were systematically made in the same order: *I/V* curve, steady-state inactivation, recovery from inactivation (HP = −120 mV and HP = −100 mV), ten min after breaking the seal.

Statistical Analysis

For each experiment, a one-way ANOVA was performed to compare mean values between groups (wild-type and chimeric channels). No transformation was applied to the data as normality and variance assumption were respected. All comparisons were done with the Dunnett's Technic and rSkM1 was defined as control group. All reported results were expressed as mean ± SEM and *P*-values $\leqslant 0.05$ were declared significant. Data were analyzed using the statistical package program SAS (SAS Institute, Cary, NC).

In some graphs, error bars were smaller than the symbol size and therefore not apparent. The best fit for the inactivation phase was determined visually using pCLAMP software v6.0 (Axon Instruments).

Recombinant DNA Constructions of Chimeric Channels

pS1S1 (pSelect-1/rSkM1) has been described (Chahine et al., 1996*a*). The pS1S1′ is a cassetted version of pS1S1 with SalI, SacI, Hpa1 and AflII sites introduced as silent mutations at nucleotides 2171, 2843, 3967 and 4568, respectively, using the following antisense oligonucleotides:

SalI 5′-TACCCAGGTCGACAAAGGGGT-3′;
SacI 5′-CACTGAAGGAGCTCAGCAGGA-3′;
HpaI 5′-CAAACAAGTTAACCCCCATGA-3′;
AflII 5′-TGTCCACCTTAAGCTGGCTCT-3′.

The underlined nucleotides are the mutation sites.

pS1H1 (pSelect-1/hH1) has been described (Chahine et al., 1996*a*). pS1H1′ is a cassetted version of pS1H1 with SplI, SalI, SacI, HpaI and AflII, introduced as silent mutation at nucleotides 1394, 2305, 2967, 4209 and 4813, respectively, using the following antisense oligonucleotides:

SplI 5′-TTTGCTCCTCGTACGCCATTGCGA-3′;
SalI 5′-TGATGGTGAGGTCGACAAACGGGTCCATG-3′;
SacI 5′-TGAAGGAGCTCAGCAGCAAGG-3′;
HpaI 5′-CAAAGAGGTTAACGCCCATGA-3′;
AflII 5′-GGCCAAGATGTTGATCTTAAGAGGACTTTGGTCATC-3′

pcDNA/LQ-4 (10.5 kb) consists of pcDNA1 (4.8 kb with HindIII and NotI ends), HindIII-SplI (1.2 kb from pS1H1′) and SplI-NotI (4.5 kb from pS1S1′) fragments. The juction sequence is (numbering is that of the parent cDNA sequence):

Met Ala Tyr Ala Glu
1390-AGT.GC/G.TAC.GCT.GAG-1789
hH1 SplI rSkM1

pcDNA/LQ-19 (11.8 kb) consists of pcDNA1 (4.8 kb with HindIII and EcoRI ends), HindIII-SacI (2.5 kb from pS1S1′), and SacI-EcoRI (4.5 kb from pS1H1′) fragments. The junction sequence is:

Leu Leu Ser Ser Phe
2834-CTG.CTG.AGC.T/CC.TTC-2976
rSkM1 SacI hH1

pcDNA/LQ-28 (10.5 kb) consists of pcDNA1 (4.8 kb with HindIII and EcoRI ends), HindIII-SalI (1.8 kb from pS1S1′), SalI-SacI (0.6 kb from pS1H1′), SacI-HpaI (1.1 kb from pS1S1′), HpaI-AflII (0.6 kb from pS1H1′), and AflII-EcoRI (1.6 kb from pS1S1′) fragments. The junctions sequences are:

Pro Phe Val Asp Leu
2165-CCC.TTT.G/TC.GAC.CTC-2313
rSkM1 SalI hH1

Leu Leu Ser Ser Phe
2962-CTG.CTG.AGC.T/CC.TTC-2848
hH1 SacI rSkM1

Gly Val Asn Leu
3961-GGG.GTT./AAC.CTC-4215
rSkM1 HpaI hH1

Ser Pro Leu Cys Val
4806-AGT.CCT.C/TT.AAG.GTG-4576
rH1 AflII rSkM1

pcDNA/LQ-9 (11.8 kb) consists of pcDNA1 (4.8 kb with HindIII and EcoRI ends), HindIII-HpaI (3.6 kb from pS1S1′), and HpaI-EcoRI (3.4 kb from pS1H1′) fragments. The junction sequence is:

Gly Val Asn Leu
3961-GGG.GTT/ACC.CTC-4215 gttaac
rSkM1 HpaI hH1

pcDNA/LQ-18 (10.8 kb) consists of pcDNA1 (4.8 kb with HindIII and NotI ends), HindIII-SacI (2.5 kb from pS1S1′), SacI-HpaI (1.2 kb from pS1H1′), and HpaI-NotI (2.3 kb from pS1S1′) fragments. The junction sequences are:

Leu Leu Ser Ser Phe
2834-CTG.CTG.AGC.T/CC.TTC-2976
rSkM1 SacI hH1

Gly Val Asn Leu
4204-GGC.GTT/AAC.TTG-3973
hH1 HpaI rSkM1

pcDNA/LQ-29 (11.1 kb) consists of pcDNA1 (4.8 kb with HindIII and NotI ends), HindIII-SalI (2.2 kb from pS1H1′), SalI-HpaI (1.8 kb from pS1S1′), HpaI-AflII (0.6 kb from pS1H1′), and AflII-NotI (1.7 kb from pS1S1′) fragments. The junction sequences are:

Phe Val Asp Leu
2305-TTT.G/TC.GAC.CTG-2179
hH1 SalI rSkM1

Gly Val Asn Leu
3961-GGG.GTT/ACC.CTC-4215 gttaac
rSkM1 HpaI hH1

Ser Pro Leu Cys Val
4806-AGT.CCT.C/TT.AAG.GTG-4576
hH1 AflII rSkM1

Results

In a previous study we showed that rSkM1 and hH1 possess important electrophysiological differences when expressed in the tsA201 cell line, such as: (i) voltage-dependence of steady-state activation, (ii) kinetics of inactivation, (iii) voltage-dependence of steady-state inactivation and (iv) kinetics of recovery from inactivation (Chahine et al., 1996*a*). We have now extended these studies to the consideration of chimeras constructed between rSkM1 and hH1 by interchanging one or two domains between the two isoforms to attempt to correlate these electrophysiological differences with regions of variation in the structure of sodium channels.

Rate of Inactivation

Families of sodium currents from cells transfected with the parental channels, rSkM1 and hH1, were recorded with a holding potential of −120 mV and 30 msec depolarizations of −80 to +60 mV in 10-mV increments (Fig. 1*A* and *C*). The decay of the sodium current after the peak is slower for hH1 than for rSkM1 (Fig. 1*B* and *D*) and has been fit with a single exponential for rSkM1 (τ_h) and two exponentials for hH1 (τ_h^{fast} and τ_h^{slow}) (Table). The relative amplitude of the fast component of hH1 was 96% at −10 mV.

To locate the portion of the channel that is responsible for the slow inactivation phenotype of hH1, we examined different chimeric constructs containing various combinations of elements of rSkM1 and hH1. Chimeras were created in which single domains of hH1 were sequentially placed into a largely rSkM1 background (LQ-4 for N-$_{ter}$D1, LQ-28 for D2, LQ-18 for D3 and LQ-9 for D4-C$_{ter.}$, Fig. 2) (N_{ter} and C_{ter} are the amino terminus and carboxyl terminus segments of the channel protein). Note that all chimeric channels reported herein show expression levels, when transfected in tsA201 cell line, comparable to that seen with the wild-type rSkM1 and hH1 sodium channels with two exceptions, LQ-18

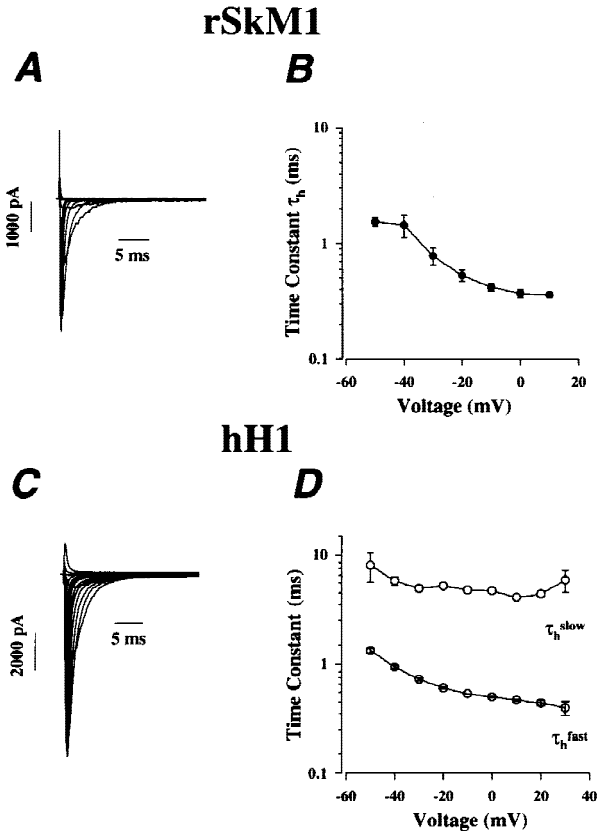

Fig. 1. Whole-cell sodium current traces from rSkM1 (*A*) and hH1 (*C*) expressed in the tsA201 cell line. Currents were recorded at a holding potential of −120 mV stepped from −80 to +60 mV during 30 msec in 10-mV increments. Sodium currents obtained at different voltages were fitted with one or two time constants and the voltage-dependence of time constant of inactivation (τ_h) for rSkM1 (*B*) and τ_h^{fast} and τ_h^{slow} for hH1 (*D*) are shown.

and LQ-28 in which we recorded smaller sodium currents for a given amount of DNA.

A typical family of sodium currents recorded from a cell transfected with LQ-9 shows slow inactivation kinetics (Fig. 2*D*) and the inactivation kinetics were best fit with two time constants (τ_h^{fast} and τ_h^{slow}) as was the case for hH1 sodium currents (Fig. 2*D* and Table). LQ-9 is a chimeric channel where N_{ter}-D1-D2-D3 are from rSkM1, D4-C_{ter} is from hH1 and the interdomain 3–4 loop (ID_{3-4}) is from hH1. Figure 3 shows one time constant fit for rSkM1, LQ-4, LQ-28, LQ-18 and LQ-29. In contrast to hH1, LQ-9 and LQ-19 where two time constants *vs.* one time constants were shown indicating that two time constants were required to fit the inactivation phase of these channels (Fig. 4). These data suggest that the slow and biphasic inactivation phenotype of hH1 is associated with D4-C_{ter} of the heart channel isoform. Corroboration for this conclusion is based on studies of LQ-19, which is composed of N_{ter}, D1 and D2 from rSkM1, and ID_{2-3}-D3-D4-C_{ter} derive from hH1). The current decays show the same slow and biphasic inactivation kinetics (Fig. 2*F*) as LQ-9 and hH1 (Fig. 2*D* and the Table) and two time constants were required to fit the decay of the current after the peak. Figure 5*A* and *B* summarize two time constants *vs.* one time constant fit for rSkM1, hH1 and the six chimeras studied.

If our conclusion is correct, introducing individual domains (D1, D2 and D3) of hH1 into a rSkM1 background should have no effect on the rSkM1 inactivation kinetics phenotype, since D4-C_{ter} derives from rSkM1 in each instance, and such is the case for chimeras LQ-4, LQ-28 and LQ-18 (Fig. 2*A, B* and *C*; Fig. 4*B, C* and *D*; Fig. 5*A* and *B* and the Table). This correlation holds true also for LQ-9 and LQ-19 (Fig. 2*D* and *F*; Fig. 4*C* and *D* and *E*,*F*; Fig. 5*A* and *B* and Table).

Steady-State Activation (G-V)

Other differences between rSkM1 and hH1 are the Boltzmann parameters representing the midpoints ($V_{1/2}$) and slope factors (K_V) of the steady-state activation *G-V* curves derived from families of currents similar to that depicted above (Fig. 1), rSkM1 ($V_{1/2}$ = −35.7 ± 2.2, K_V = 7.4 ± 0.3) and hH1 ($V_{1/2}$ = −53.6 ± 2, K_V = 6.4 ± 0.9). The reversal potentials of all the sodium currents (wild-type and chimeric channels) were in accord with the value expected from the Nernst equation: $E_{rev} = (RT/zF)\ ln\ \{Na\}_{out}/[Na]_{in}$ = 37 mV, where $\{Na\}_{out}$ = 150 mM and $\{Na\}_{in}$ = 35 mM. This confirms that the currents studied are carried by sodium ions. The current-voltage (*I/V*) and *G-V* relationships for hH1, rSkM1 and six chimeric sodium channels show that Boltzmann equation fits for the data from chimeric channels have no statistical differences when compared to rSkM1 (Fig. 5*C*, Table). No simple correlation in steady-state activation parameters with the structures of the chimeras is apparent.

Steady-State Inactivation (h∞)

Steady-state inactivation was studied by a two-pulse protocol with 500 msec depolarizing prepulses from a holding potential of −140 mV stepped from −140 to −30 mV in 10 mV increments followed by a −30 mV test pulse. Each experiment was fitted with a Boltzmann equation which provides half-inactivation ($V_{1/2}$) and the slope factor (K_V) parameters for each channels studied (Fig. 6*A* and the Table). hH1 ($V_{1/2}$ = −100 ± 1.4 mV, K_V = 5.7 ± 0.2) inactivates at more negative voltages than rSkM1 ($V_{1/2}$ = −88.2 ± 2.1 mV, K_V = 6.0 ± 0.2). These values differ from those previously reported due to liquid junction potential corrections in the present publication: rSkM1, $V_{1/2}$ = −76 mV, K_V = 5.2; and hH1, $V_{1/2}$ = −95.3 mV, K_V = 7.5 (Chahine et al., 1996*a*). The results with the chimeric channels show that the Boltz-

Table. Activation and inactivation parameters for hH1, rSkM1 and chimeric sodium channels

	Steady-state activation (mV)	Time constant of inactivation τ_h (msec)(−10 mV)	Amplitude coefficient (−10 mV)	Steady-state inactivation (mV)	Recovery from inactivation (msec)		Ratio $\tau_{rec}^{-100}/\tau_{rec}^{-120}$	*n*
					τ_{rec}:−100 mV	τ_{rec}:−120 mV		
rSkM1	$V_{1/2}$ = −35.7 ± 2.2*	τ_h: 0.4 ± 0.1		$V_{1/2}$ = −88.2 ± 2.1*	11.6 ± 1.2*	6.2 ± 0.3*	1.88	6
	k_v = 7.4 ± 0.3			k_v = 6 ± 0.2				
hH1	$V_{1/2}$ = −53.6 ± 2	τ_h^{fast}: 0.5	0.96	$V_{1/2}$ = −100.0 ± 1.4	51.9 ± 5.8	12.7 ± 0.4	4.09	6
	K_v = 6.4 ± 0.9	τ_h^{slow}: 4.8 ± 0.1		k_v = 5.7 ± 0.2				
LQ-4	$V_{1/2}$ = −38.7 ± 3.4*	τ_h: 0.6 ± 0.1		$V_{1/2}$ = −91.5 ± 1.6*	12.1 ± 0.6*	4.6 ± 0.2*	2.64	6
	k_v = 7.3 ± 0.7			k_v = 6.3 ± 0.4				
LQ-28	$V_{1/2}$ = −27.4 ± 1.6*	τ_h: 0.5 ± 0.1		$V_{1/2}$ = −82.7 ± 0.5*	13.9 ± 0.8*	5.4 ± 0.2*	2.57	6
	k_v = 9.3 ± 0.3			k_v = 4.6 ± 0.2				
LQ-18	$V_{1/2}$ = −28.1 ± 1.9*	τ_h: 0.6 ± 0.1		$V_{1/2}$ = −92.4 ± 0.7*	12.2 ± 1.1*	7.7 ± 0.3*	1.58	5
	k_v = 10.4 ± 0.9			k_v = 6.4 ± 0.2				
LQ-9	$V_{1/2}$ = −32.2 ± 2.7*	τ_h^{fast}: 0.6 ± 0.1	0.94	$V_{1/2}$ = −80.1 ± 2.9*	8.8 ± 0.7*	3.8 ± 0.3*	2.23	6
	k_v = 8.2 ± 0.6	τ_h^{slow}: 5.5 ± 0.5		k_v = 5.6 ± 0.5				
LQ-29	$V_{1/2}$ = −20.0 ± 1.6*	τ_h: 0.7 ± 0.1		$V_{1/2}$ = −88.0 ± 1.8*	13.93 ± 1.1*	6.2 ± 1.1*	2.25	5
	k_v = 10.6 ± 0.5			k_v = 5.7 ± 0.3				
LQ-19	$V_{1/2}$ = −26.9 ± 2.1*	τ_h^{fast}: 0.7 ± 0.1	0.95	$V_{1/2}$ = −85.4 ± 1.9*	14.3 ± 0.9*	6.2 ± 0.4*	2.00	4
	k_v = 10.3 ± 0.4	τ_h^{slow}: 4.2 ± 0.4		k_v = 6.4 ± 0.5				

* $P < 0.05$ compared to hH1.

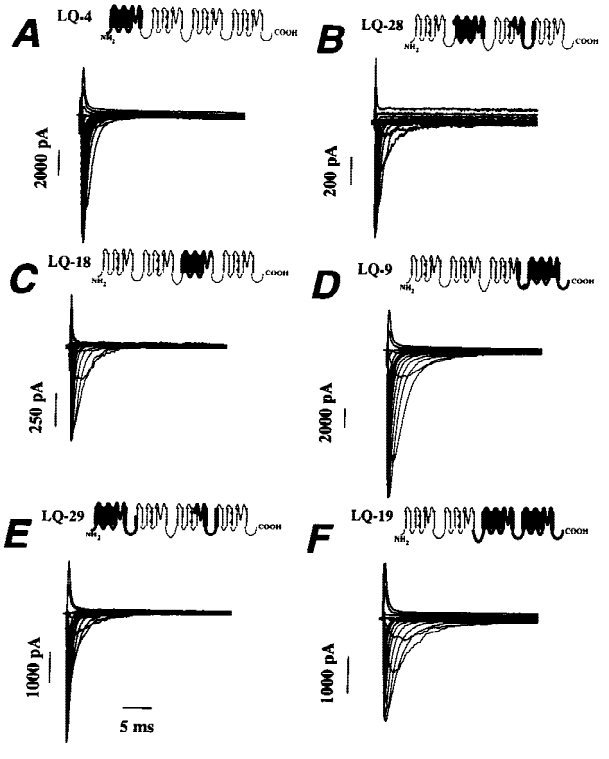

Fig. 2. Whole-cell sodium current traces from the chimeras LQ-4 (*A*), LQ-28 (*B*), LQ-18 (*C*), LQ-9 (*D*), LQ-29 (*E*) and LQ-19 (*F*) expressed in the tsA201 cell line. Currents were recorded at a holding potential of −120 mV stepped from −80 to +60 mV during 30 msec in 10-mV increments. Schematic representation of the corresponding chimeras illustrating the origin of rSkM1 and hH1 of the four domains on the top. hH1 domains are shown dark and rSkM1 domains are shown light.

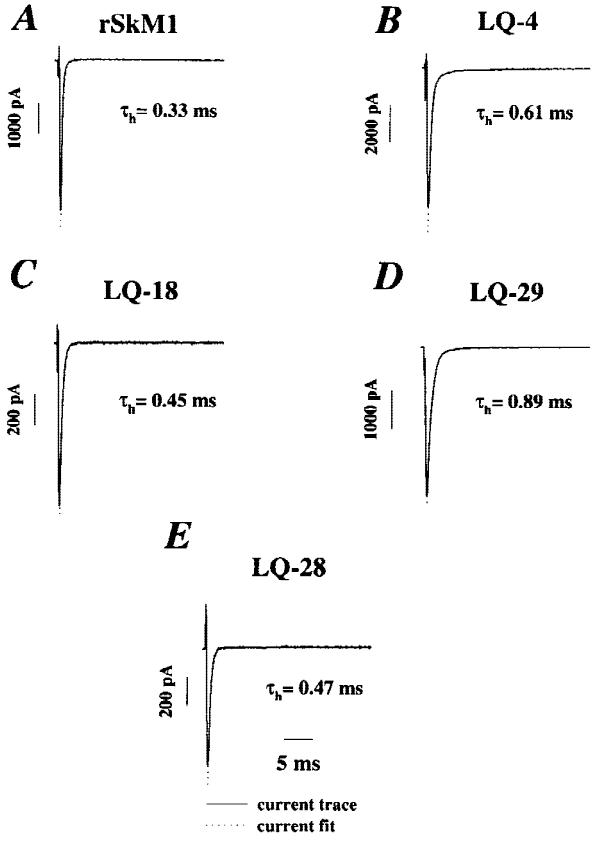

Fig. 3. Whole cell inward sodium currents recorded at −10 mV test pulse from −120 mV holding potential and fitted by single exponential function for wild-type rSkM1 and chimeric channels created between rSkM1 and hH1 {LQ-4 (B), LQ-18 (C), LQ-29 (*D*) and LQ-28 (E)}. τ_h represent the time constant of the exponential fit.

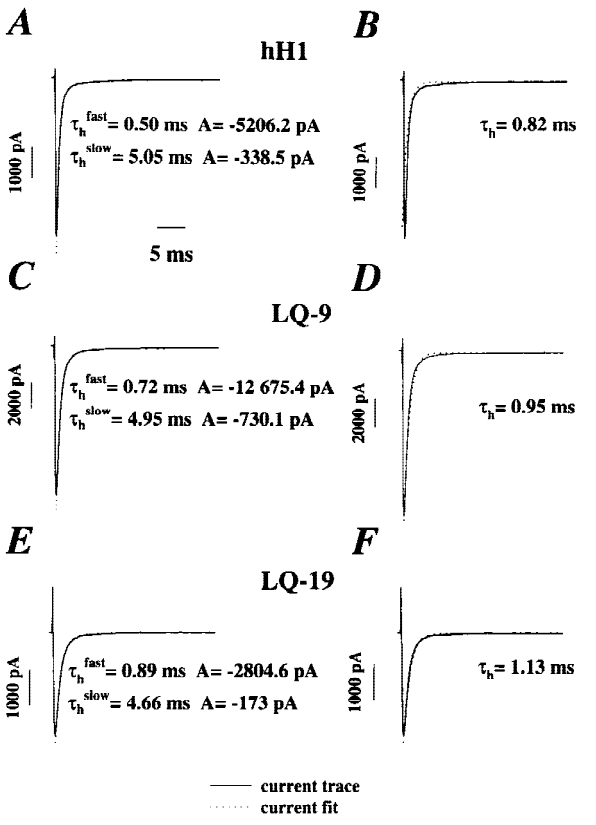

Fig. 4. Whole-cell inward sodium currents elicited by a test pulse of −10 mV from a holding potential of −120 mV of hH1 (*A* and *B*), LQ-9 (*C* and *D*) and LQ-19 (*E* and *F*). Currents were fitted with 1 time constant exponential function (right) (τ_h represent the time constant of the exponential fit) *vs.* 2 time constants exponential function (left) where the time constants values and amplitude associated with fast (τ_h^{fast}) and slow (τ_h^{slow}) were indicated.

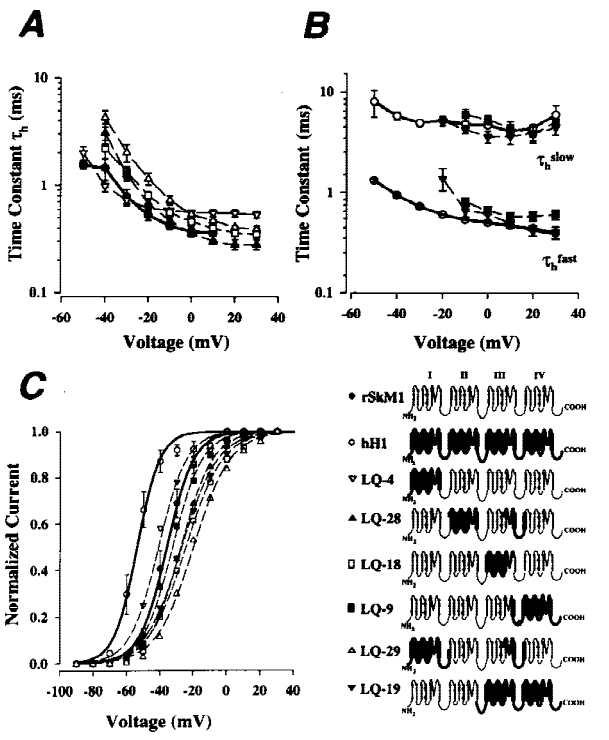

Fig. 5. (*A*) and (*B*) Voltage-dependence of the time constant of inactivation for rSkM1, hH1 and the chimeras. Current decay after the peak at different voltages was fitted with a single exponential (τ_h) for rSkM1, LQ-4, LQ-18, LQ-28 and LQ-29. For hH1, LQ-19 and LQ-9, the falling phase of each record needed to be fit with two exponentials (τ_h^{fast} and τ_h^{slow}). (*C*) Normalized current activation curves of hH1, rSkM1 and chimeric channels formed from rSkM1 and hH1 versus voltage (mean ± SEM). For clarity the error bars were omitted from all the chimeras.

mann parameters are comparable to those of rSkM1 and are statistically different from those obtained with hH1.

Recovery from Inactivation

The recovery from inactivation was studied at two different holding potentials, −120 and −100 mV with a two-pulse protocol (Fig. 6*B* and *C*). A prepulse of 40 msec depolarization to −20 mV was followed at various time interval (Δt) with a 40 msec test pulse to −20 mV (Fig. 6*B* and *C*). The amplitude of the test-pulse currents were normalized with the prepulse currents and the results were fit with a single exponential. At a holding potential of −100 mV, rSkM1 has a τ_{rec} value of 11.6 ± 1.2 msec while hH1 has one of 51.9 ± 5.8 msec. At a holding potential of −120 mV (Fig. 6*B*), the recovery from inactivation is faster for wild-type channels compared to that observed at −100 mV (Fig. 6*C*, Table). Thus at the same holding potential (either −120 or −100 mV), hH1 recovers from inactivation 4.5-fold more slowly than rSkM1. The τ_{rec} values for the chimeras studied fell within the range of 8.8 to 14.3 msec closely bracketing the value for rSkM1 at −100 mV. Except for smaller time constants, a similar situation applies for a holding potential of −120 mV (Table). The ratio of the recovery time constants at the two voltages ($\tau_{rec}^{-100}/\tau_{rec}^{-120}$) gives a crude measure of the voltage-dependence of the kinetics of recovery from inactivation and a comparison of these values for the chimeras (Table) shows that the behavior of the chimeras is also similar to that of rSkM1, less voltage-dependent, compared to that of hH1.

Discussion

In native tissues, voltage-gated sodium channels from heart, brain and skeletal muscle have different pharmacological and electrophysiological properties (Backx et al., 1992; Frelin et al., 1986; Kirsch & Brown, 1989; Ravindran, Schild & Moczydlowski, 1991; Schild & Moczydlowski, 1991; Arreola, Spires & Begenisich,

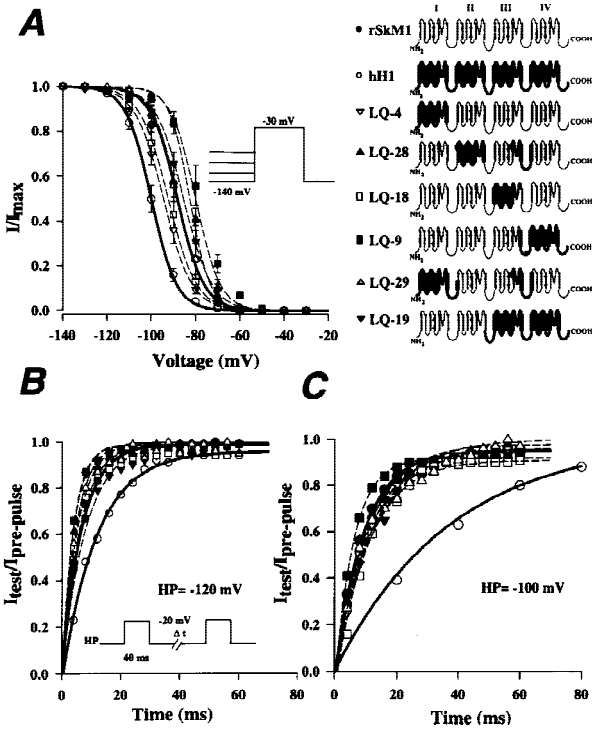

Fig. 6. (*A*) Voltage-dependence of steady-state inactivation ($h\infty$) of rSkM1, hH1 and the chimeric channels at −30 mV triggered by 500-msec prepulse ranged from −140 to −30 mV. The curve was fitted to a Boltzmann distribution $I/I_{max} = 1/1+\exp((V-V_{1/2})/K_V)$ with given $V_{1/2}$ and K_V values. (*B*) and (*C*) Time course of recovery from inactivation for rSkM1, hH1 and the chimeric channels was studied using a two-pulse duration at −20 mV measured at various interpulse intervals (Δt) of either 4 msec or 20 msec (hH1 at HP = −100 mV) (*C*). The solid line shows the fit of the data using the following equation $I_{test}/I_{prepulse} = 1\text{-}\exp(-t/\tau_{rec})$.

1993). The α-subunits of rat skeletal muscle and human heart channel isoforms, when expressed in mammalian cell lines, show similar electrophysiological differences as those seen in tissues. These distinguishable behaviors involve voltage-dependence of steady-state activation and inactivation and the kinetics of and recovery from inactivation (Chahine et al., 1996*a*; Wang et al., 1996). These data for expressed channels suggest that the electrophysiological differences are due to structural differences that are located within the α-subunits of the voltage-gated sodium channels and are not due to other modulating factors or auxiliary subunits. We chose to examine whether a given electrophysiological difference could be correlated with a restricted portion of the channel, perhaps a single domain or less of the α-subunit. Based on the known structure of the α-subunits of hH1 (Gellens et al., 1992) and rSkM1 (Trimmer et al., 1989), we constructed a panel of chimeric channels. All of the chimeras were successfully expressed and the efficiency of the expression was, in general, comparable to the wild-type channels.

Chimeric channels have been very useful for studying the structural basis for localized determinants of phenotype, for example, the difference between low and high affinity TTX or divalent metal ion binding (Backx et al., 1992; Chen et al., 1992; Satin et al., 1992). Such an analysis may reveal the segments in the channel protein directly involved in the phenomenon or indirectly, for example, in the transduction of a structural change propagated from a distal site. In the latter case the structural change may be the same but the transducer may differ from isoform to isoform accounting for differences in phenotype. In cases in which a simple correlation does not result from an analysis of chimeric proteins, it may be evidence that multiple portions of the protein determine that attribute. In the present studies we have used two distantly related sodium channels that exhibit many differences in phenotype and possess an overall identity ~50% at the amino acid level. However, the overall organization and structure of the pair of channel isoforms are similar. For example, within the more conserved segments, such as S4, which is thought to be involved in voltage-dependent activation, the number of charged residues and their arrangement in the primary sequence do not differ between the isoforms. Indeed, there are only two conservative differences in S4 segments (rSkM1/hH1): Thr^{232}/Ser^{232} in D1 and Val^{1451}/Ile^{1633} in D4. Similarly, the ID3-4 loops are very highly conserved with eight differences in a total of 53 amino acids (*see below*). The availability of rSkM1 and hH1 cDNAs presented us with an opportunity to elucidate which regions of the channels might account for differences in activation and inactivation between the isoforms.

Kinetics of Inactivation

Although the kinetics of activation of the chimeric channels do not appear to be grossly different from that of the parent channels, hH1 and rSkM1 (Fig. 1) the kinetics of inactivation show substantial differences among the various constructs. As noted earlier, in order to fit the decay phase of the sodium current, for rSkM1 a single exponential was needed with a time constant of inactivation, τ_h. In contrast, for hH1, two exponentials were necessary to fit the current inactivation phase, τ_h^{fast} and τ_h^{slow}. For the chimeras that possess rSkM1-like inactivation kinetics (LQ-4, LQ-28, LQ-18 and LQ-29, which have D4-C_{ter} from rSkM1) only a single exponential was needed but for those chimeras exhibiting hH1-like (LQ-19 and LQ-9, which have D4-C_{ter} from hH1), two exponentials were required (Table). Note particularly that the source of the ID3-4 loop, which is thought to contain the inactivation particle, is not correlated with the phenotypic differences in inactivation kinetics when we compare the six channel chimeras. This result is in agree-

ment with previous studies with other chimeric channels (Chahine et al., 1996*a*).[1]

Thus, we are drawn to the conclusion that a major determinant of the difference in inactivation rate resides in D4-C_{ter} (Fig. 3). This is consistent with the following observations: (i) A tendency for naturally occurring mutations in humans to be located more frequently in D4: these mutations slow macroscopic inactivation and, in some cases, are associated with increased frequency of channel reopening (Zhou et al., 1991; Chahine et al., 1994). The electrophysiological consequences of these mutations have been implicated in the pathogenesis of hyperkalemic familial periodic paralysis, paramyotonia congenita, and myotonia congenita. (ii) Mutations in which the basic residues in S4D4 are replaced with neutral or acidic residues have a unique effect on the kinetics and voltage-dependence of inactivation (Chahine et al., 1994; Yang & Horn, 1995; Chen et al., 1996; Yang et al., 1996) compared with similar mutations in the S4 segments of D1, D2 and D3 (Chen et al., 1996). (iii) Amino acid replacements in the S4-S5 loop of D4 have profound effects on the kinetics of inactivation (Tang, Kallen & Horn, 1996). However the role of the C-terminal in fast inactivation of voltage-gated sodium channels remains to be established.

We interpret these results as indicating that D4-C_{ter} is the main structural region differentially affecting the rates of inactivation in rSkM1 and hH1. Previously it was suggested that the positioning of the inactivation particle optimally at various extents of depolarization depends on a linkage between the inactivation particle and voltage-sensors, especially S4D4, located in the core of the channel (O'Leary et al., 1995). We anticipate that a higher resolution analysis of the differences in the structures of D4-C_{ter} between the channel isoforms will establish the basis for the kinetic differences. Candidate sites cannot include S4-S5D4, which are identical between the two channels, but might embrace Ile^{1627} in S4D4 of hH1, which is replaced by Val^{1451} in rSkM1, or Ile^{1407}, which is substituted by Gln^{1589} in S2-S3D4.

Our conclusion regarding D4-C_{ter} does not mean that other portions of the channel are not involved in inactivation, but merely that they are not differentially involved. Thus, if S4-S5 loops of other domains contribute elements to a hypothetical receptor for the inactivation particle located in ID3-4 (Stühmer et al., 1989; West et al., 1992; Patton et al., 1992; Hartmann et al., 1994; O'Leary et al., 1995; Bennett et al., 1995; Dumaine et al., 1996), their effects are comparable whether the segments derive from hH1 or rSkM1 or both.

[1]A previous study of inactivation of rat skeletal muscle/heart chimeric channels is deemed unsatisfactory because expression in *Xenopus* oocytes results in abnormal inactivation kinetics for rSkM1 (Chen et al., 1992).

Voltage-Dependence of Activation

In the past we and others have found that kinetic studies, such as those described above, have been more readily interpretable than voltage dependencies and slope factors of steady-state activation and inactivation curves. This has proven to be the case in terms of the $V_{1/2}$ and slope factor of the Boltzmann parameters of the G-V curves for the chimeras. The $V_{1/2}$ values of chimeric channels are not statistically different from those of rSkM1. The bulk of these observations supports a view of channel structure in which many different areas (probably the S4 segments of the four domains, which are believed to act as voltage sensors) are involved with activation (Yang & Horn, 1995; Chen et al., 1996; Yang et al., 1996) and the four S4 segments account for the G-V curve.

Voltage-Dependence of Inactivation (h_∞)

Steady-state inactivation characteristics also seem to be determined by more than one domain since none of the chimeras behaved similar to hH1, which inactivates at more negative voltage than rSkM1 and the chimeric channels. Those differences in the steady-state inactivation midpoints cannot be attributed to a time-dependent shift observed with different sodium channels (Hanck & Sheets, 1992; Wang et al., 1996) because this was carefully controlled. Instead, our results point to structural differences between hH1 and rSkM1. It is noteworthy that plots of midpoints and slope factors of steady-state inactivation *vs.* G-V also show no correlation among the chimeras despite the fact that activation and inactivation are thought to be coupled in wild-type sodium channels (Aldrich, Corey & Stevens, 1983).

Recovery from inactivation was studied at two different holding potentials. At a holding of −100 mV all the sodium channels studied were slower in their recovery from inactivation than at a holding potential of −120 mV. For a giving holding potential, hH1 recovers much more slowly than rSkM1 and all the chimeras. The voltage-dependence of the rate of recovery from inactivation obtained from the ratio of τ_{rec} values at −100 and −120 mV (Table) are also rSkM1-like for all the chimeras. Thus, if D2 and/or D3 is from rSkM1, the phenotype is rSkM1-like. This conclusion is consistent with that obtained from studies with a chimera in which both D2 and D3 from rSkM1 were inserted into a hH1 background (LQ-5) because this chimera also showed a rSkM1 phenotype for rate of recovery (Chahine et al., 1996*a*). For this electrophysiological property, since none of the chimeras acted as hH1, more than one domain seems to be incriminated.

Additional studies are underway to provide a higher resolution analysis for the structural basis for the influence of D4-C_{ter} on inactivation kinetics.

References

Aldrich, R.W., Corey, D.P., Stevens, C.F. 1983. A reinterpretation of mammalian sodium channel gating based on single channel recording. *Nature* **306:**436–441

Auld, V.J., Goldin, A.L., Krafte, D.S., Catterall, W.A., Lester, H.A., Davidson, N., Dunn, R.J. 1990. A neutral amino acid change in segment IIS4 dramatically alters the gating properties of the voltage-dependent sodium channel. *Proc. Natl. Acad. Sci. USA* **87:**323–327

Arreola, J., Spires, S., Begenisich, T. 1993. Na^+ channels in cardiac and neuronal cells derived from a mouse embryonal carcinoma cell line. *J. Physiol.* **472:**289–303

Backx, P.H., Yue, D.T., Lawrence, J.H., Marban, E., Tomaselli, G.F. 1992. Molecular Localization of an ion-binding site within the pore of mammalian sodium channels. *Science* **257:**248–251

Bennett, P.B., Valenzuela, C., Chen L.-Q., Kallen, R.G. 1995. On the molecular nature of the lidocaine receptor of cardiac Na^+ channels. Modification of block by alterations in the α-subunit III-IV interdomain. *Circ. Res.* **77:**584–592

Catterall, W.A. 1992. Cellular and molecular biology of voltage-gated sodium channels. *Physiol. Rev.* **72:**S15–S48

Catterall, W.A. 1993. Structure and modulation of Na^+ and Ca^{2+} channels. *Ann. N.Y. Acad. Sci.* **707:**1–19

Chahine, M., Deschênes, I., Chen, L.-Q., Kallen, R.G. 1996*a*. Electrophysiological characteristics of cloned skeletal and cardiac muscle sodium channels expressed in tsA201 cells. *Am. J. Physiol.* **40:**H498–H506

Chahine, M., George, A.L., Jr., Zhou, M., Ji, S., Sun, W., Barchi, R.L., Horn, R. 1994. Sodium channel mutations in paramyotonia congenita uncouple inactivation from activation. *Neuron* **12:**281–294

Chahine, M., Plante, E., Kallen, R.G. 1996*b*. Sea anemone toxin (ATX II) modulation of heart and skeletal muscle sodium channel α-subunits expressed in tsA201 cells. *J. Membrane Biol.* **152:**39–48

Chen, L.-Q., Chahine, M., Kallen, R.G., Barchi, R.L., Horn, R. 1992. Chimeric study of sodium channels from rat skeletal and cardiac muscle. *FEBS Lett.* **309:**253–257

Chen, L.Q., Santarelli, V., Horn, R., Kallen, R.G. 1996. A unique role for the S4 segment of domain 4 in the inactivation of sodium channels. *J. Gen. Physiol.* **108:**549–556

Cohen, S.A., Mello, C., Yang, J. 1993. Developmental and regional expression of RH1 mRNA in the rat heart. *Biophys. J.* **64:**A92 Abstr

Dumaine, R., Wang, Q., Keating, M.T., Hartmann, H.A., Schwartz, P.J., Brown, A.M., Kirsch, G.E. 1996. Multiple mechanisms of Na^+ channel-linked long-QT syndrome. *Circ. Res.* **78:**916–924

Frelin, C., Cognard, C., Vigne, P., Lazdunski, M. 1986. Tetrodotoxin-sensitive and tetrodotoxin-resistant Na^+ channels differ in their sensitivity to Cd^{2+} and Zn^{2+}. *Eur. J. Pharmacol.* **122:**245–250

Gellens, M.E., George, A.L., Jr., Chen, L., Chahine, M., Horn, R., Barchi, R.L., Kallen, R.G. 1992. Primary structure and functional expression of the human cardiac tetrodotoxin-insensitive voltage-dependent sodium channel. *Proc. Natl. Acad. Sci. USA* **89:**554–558

Hamill, O.P., Marty, A., Neher, E., Sakmann, B., Sigworth, F.J. 1981. Improved patch-clamp techniques for high-resolution current recording from cells and cell-free membrane patches. *Pfluegers Arch.* **391:**85–100

Hanck, D.A., Sheets, M.F. 1992. Time-dependent changes in kinetics of Na^+ current in single canine cardiac Purkinje cells. *Am. J. Physiol.* **262:**H1197–H1207

Hartmann, H.A., Tiedeman, A.A., Chen, S.-F., Brown, A.M., Kirsch, G.E. 1994. Effects of III-IV linker mutations on human heart Na^+ channel inactivation gating. *Circ. Res.* **75:**114–122

Heinemann, S.H., Terlau, H., Stühmer, W., Imoto, K., Numa, S. 1992. Calcium channel characteristics conferred on the sodium channel by single mutations. *Nature* **356:**441–443

Hodgkin, A.L., Huxley, A.F. 1952. A quantitative description of membrane current and its application to conduction and excitation in nerve. *J. Physiol* **117:**500–544

Jurman, M.E., Boland, L.M., Liu, Y., Yellen, G. 1994. Visual identification of individual transfected cells for electrophysiology using antibody-coated beads. *Biotechniques* **17:**876–881

Kallen, R.G., Cohen, S.A., Barchi, R.L. 1993. Structure, function and expression of voltage-dependent sodium channels. *Mol. Neurobiol.* **7:**383–428

Kirsch, G.E., Brown, A.M. 1989. Kinetic properties of single sodium channels in rat heart and rat brain. *J. Gen. Physiol.* **93:**85–89

Larsson, H.P., Baker, O.S., Dhillon, D.S., Isacoff, E.Y. 1996. Transmembrane movement of the *Shaker* K^+ channel S4. *Neuron* **16:**387–397

Makielski, J.C., Limberis, J.T., Chang, S.Y., Fan, Z., Kyle, J.W. 1996. Coexpression of β1 with cardiac sodium channel α subunits in oocytes decreases lidocaine block. *Mol. Pharmacol.* **49:**30–39

Makita, N., Bennett, P.B., George, A.L., Jr. 1996. Molecular determinants of β1 subunit-induced gating modulation in voltage-dependent Na^+ channels. *J. Neurosci.* **16:**7117–7127

Makita, N., Bennett, P.B., George, A.L., Jr. 1994. Voltage-gated Na^+ channel β1 subunit mRNA expressed in adult human skeletal muscle, heart, and brain is encoded by a single gene. *J. Biol. Chem.* **269:**7571–7578

Margolskee, R.F., McHendry-Rinde, B., Horn, R. 1993. Panning transfected cells for electrophysiological studies. *Biotechniques* **15:**906–911

Noda, M. 1993. Structure and function of sodium channels. *Ann. N.Y. Acad. Sci.* **707:**20–37

Nuss, H.B., Chiamvimonvat, N., Pérez-García, M.T., Tomaselli, G.F., Marbán, E. 1995*a*. Functional association of the β1 subunit with human cardiac (hH1) and rat skeletal muscle (μ1) sodium channel α subunits expressed in *Xenopus* oocytes. *J. Gen. Physiol.* **106:**1171–1191

Nuss, H.B., Tomaselli, G.F., Marbán, E. 1995*b*. Cardiac sodium channels (hH1) are intrinsically more sensitive to block by lidocaine than are skeletal muscle (μ1) channels. *J. Gen. Physiol.* **106:**1193–1209

O'Leary, M.E., Chen, L.-Q., Kallen, R.G., Horn, R. 1995. A molecular link between activation and inactivation of sodium channels. *J. Gen. Physiol.* **106:**641–658

Patton, D.E., West, J.W., Catterall, W.A., Goldin, A.L. 1992. Amino acid residues required for fast Na^+-channel inactivation: charge neutralizations and deletions in the III-IV linker. *Proc. Natl. Acad. Sci. USA* **89:**10905–10909

Pérez-García, M.T., Chiamvimonvat, N., Marban, E., Tomaselli, G.F. 1996. Structure of the sodium channel pore revealed by serial cysteine mutagenesis. *Proc. Natl. Acad. Sci. USA* **93:**300–304

Ravindran, A., Schild, L., Moczydlowski, E. 1991. Divalent cation selectivity for external block of voltage-dependent Na^+ channels prolonged by batrachotoxin. Zn^{2+} induces discrete substates in cardiac Na^+ channels. *J. Gen. Physiol.* **97:**89–115.

Satin, J., Kyle, J.W., Chen, M., Bell, P., Cribbs, L.L., Fozzard, H.A., Rogart, R.B. 1992. A mutant of TTX-resistant cardiac sodium channels with TTX-sensitive properties. *Science* **256:**1202–1205

Schild, L., Moczydlowski, E. 1991. Competitive binding interaction between Zn^{2+} and saxitoxin in cardiac Na^+ channels. Evidence for a sulfhydryl group in the Zn^{2+}/saxitoxin binding site. *Biophys. J.* **59:**523–537

Stühmer, W., Conti, F., Suzuki, H., Wang, X., Noda, M., Yahagi, N., Kubo, H., Numa, S. 1989. Structural parts involved in activation and inactivation of the sodium channel. *Nature* **339:**597–603

Tang, L., Kallen, R.G., Horn, R. 1996. Role of an S4-S5 linker in sodium channel inactivation probed by mutagenesis and a peptide blocker. *J. Gen. Physiol.* **108:**89–104

Trimmer, J.S., Cooperman, S.S., Tomiko, S.A., Zhou, J., Crean, S.M., Boyle, M.B., Kallen, R.G., Sheng, Z., Barchi, R.L., Sigworth, F.J., Goodman, R.H., Agnew, W.S., Mandel, G. 1989. Primary structure and functional expression of a mammalian skeletal muscle sodium channel. *Neuron* **3:**33–49

Tsushima, R.G., Li, R.A., Backx, P.H. 1997. Altered ionic selectivity of the sodium channel revealed by cysteine mutations within the pore. *J. Gen. Physiol.* **109:**463–475

Wang, D.W., George, A.L., Jr., Bennett, P.B. 1996. Comparison of heterologously expressed human cardiac and skeletal muscle sodium channels. *Biophys. J.* **70:**238–245

West, J.W., Patton, D.E., Scheuer, T., Wang, Y., Goldin, A.L., Catterall, W.A. 1992. A cluster of hydrophobic amino acid residues required for fast Na^+-channel inactivation. *Proc. Natl. Acad. Sci. USA* **89:**10910–10914

Westenbroek, R.E., Merrick, D.K., Catterall, W.A. 1989. Differential subcellular localization of the R_I and R_{II} Na^+ channel subtypes in central neurons. *Neuron* **3:**695–704

Yang, N.B., George, A.L., Jr., Horn, R. 1996. Molecular basis of charge movement in voltage-gated sodium channels. *Neuron* **16:**113–122

Yang, N.B., Horn, R. 1995. Evidence for voltage-dependent S4 movement in sodium channels. *Neuron* **15:**213–218

Yang, J.S., Sladky, J., Kallen, R.G., Barchi, R.L. 1991. mRNA transcripts encoding the TTX sensitive and insensitive forms of the skeletal muscle sodium channel are independently regulated after denervation. *Neuron* **7:**421–427

Zhou, J., Potts, J.F., Trimmer, J.S., Agnew, W.S., Sigworth, F.J. 1991. Multiple gating modes and the effect of modulating factors on the μl sodium channel. *Neuron* **7:**775–785